Deriner Hydropower Scheme – Geotechnical Issues and the Particular Case of the Spillway Tunnels Design and Construction

C. Cekerevac & A. Wohnlich
STUCKY SA, Renens, Switzerland

Ph. Bellwald
Former with STUCKY SA, Independent Consultant, Aigle, Switzerland

ABSTRACT: The paper addresses some geotechnical issues related to the construction of the Deriner dam and HEPP. Design considerations and rock stabilization measures are presented for the excavations which took place in a highly fractured and weathered rock mass prevailing on site. Particularly, the shallow excavations for the overflow spillways tunnels are discussed. These present huge openings that are 12 m wide and 18 m high in portal areas, with an overburden of approximately 20 m, for which numerical finite element analysis and structural discontinuity analysis have been performed to ensure safe excavation process and future operation.

1 INTRODUCTION

The Deriner hydropower scheme, which is currently under construction, is located in the north-eastern Black sea region of Turkey. It is a part of the Çoruh River regulation plan that will include 10 dams in total. It encompasses a 249 m high, double curvature arch dam with crest length of 720 m with all classic appurtenant structures and an underground powerhouse complex, which has been excavated on the right bank of the Çoruh River at a depth of approximately 100 m. The powerhouse has a width of 20 m, length of 126 m and a height of 45 m and will have four vertical Francis units with an installed production capacity of 670 MW. Two gated spillway tunnels have been designed to evacuate a 2250 m^3/s flow. In addition, 8 orifice spillways have been designed to ensure the evacuation of a maximum flood of 10'110 m^3/s.

Deriner Dam, which is the 1st key element in the Çoruh River development plan, will be amongst the very highest dams in the world and highest in Turkey in the class of thin arch dams with double curvature. The dam will have a yearly production of 2300 GWh electric energy with a storage volume of 1969×10^6 m³.

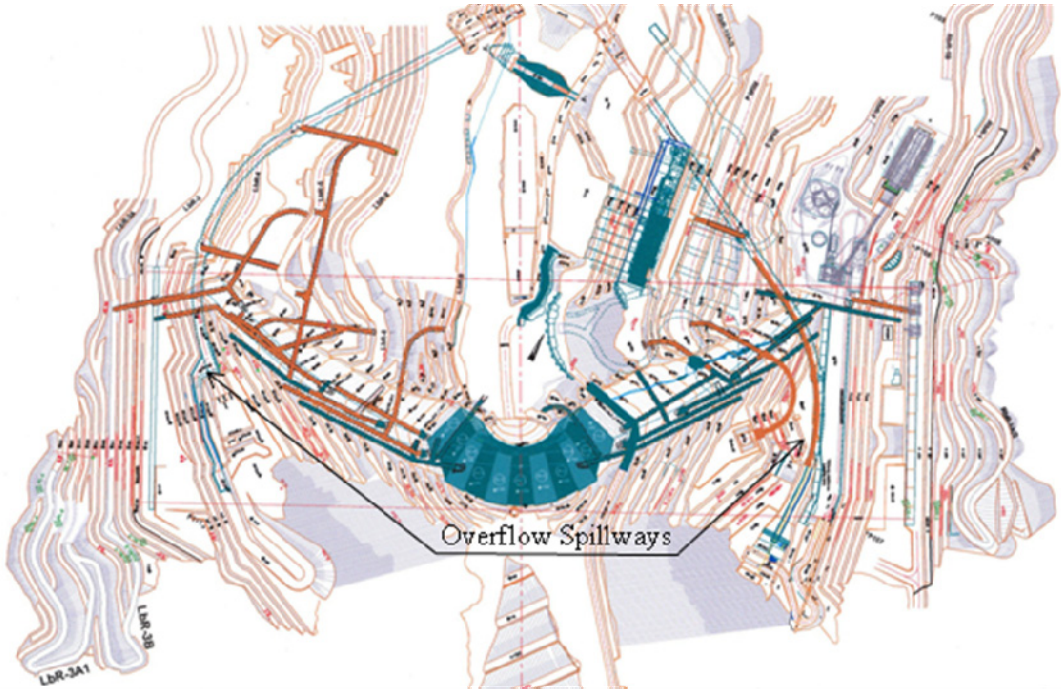

Figure 1. Layout of the Deriner HEPP.

Figure 2. Deriner HEPP, state of construction in December 2008.

2 GEOLOGICAL SET-UP OF THE DAM SITE

The rock mass at the Deriner site is mainly composed of granodiorite intruded by diabase dykes, which are generally very suitable for the foundation of an arch dam. Nevertheless, the upper layer of the rock is decompressed and heavily jointed, which means that it has to be excavated so as to ensure sound rock for the dam foundations. Since both rock types encountered on the site, diabase and granodiorite, are quite homogeneously distributed over the site and show similar properties of intact rock, there is no need to specifically take into account the lithology in defining the design values of intact rock parameters.

2.1 *Strength of the intact rock*

Strength of the intact rock has been assessed by analysing the results of the unconfined compression tests and the results of the triaxial tests. Unconfined compressive strength (UCS, or σ_{ci}) measured on dry and saturated samples differs according to the location where the samples were taken, and to the petrographic origin of the rock (Table 1).

Both rock types seem to exhibit homogeneous strength with lower values at the right bank. As expected for such crystalline rocks, saturation of the samples does not affect much the strength, except maybe for the diabase in the left bank, which loses about 20% of its strength with saturation.

Table 1: Average unconfined compressive strengths.

σ_{ci} [MPa]	Dry samples		Saturated samples	
	Diabase	Granodiorite	Diabase	Granodiorite
Left bank	97.4 ± 45.4	93.5 ± 25.8	78.7 ± 59.2	90.5 ± 25.4
Right bank	74.9 ± 25.3	73.8 ± 25.6	68.2 ± 32.6	68.7 ± 30.4

In addition to that, twenty two (22) triaxial tests have been performed on 76 mm rock cores, among which only one sample was diabase, the others being granodiorite. Table 2 summarises the results of these tests for both banks in terms of the Mohr-Coulomb shear strength peak parameters (apparent cohesion c_i [MPa] and friction angle ϕ_{pi} [°]) and the corresponding calculated UCS (σ_{ci}).

Table 2: Average parameters inferred from triaxial tests.

	Apparent c_i [MPa]	ϕ_{pi} [°]	σ_{ci} [MPa]
Left bank	45.9 ± 18.0	37.9 ± 7.84	184 ± 48.4
Right bank	21.1 ± 17.5	42.6 ± 9.00	88.8 ± 73.0

Whereas the average friction angles measured in the left and right banks are comparable, the average cohesion in the left bank is much higher, which has a dramatic effect on the calculated UCS values. Although the total number of strength tests performed on intact rock is low, it appears again that the rock in the left bank is stronger than the material in the right bank.

Considering the above, the following UCS values have been recommended as design values for dry rock. They have been used in building models for the shear strength of the jointed rock mass and in classifying this latter:

- Left bank: σ_{ci} = 120 MPa;
- Right bank: σ_{ci} = 80 MPa.

In order to measure the rock's tensile strength (σ_{ti}), Brazilian tests have been carried out. These tests are aimed at gaining a better understanding of the behaviour of the rock at low stress level. In contrast to compressive strength, tensile strength values are homogeneous in both banks. However, the difference between the two litholigic types is now noticeable, strength of diabase being higher than of granodiorite. The mean ratio between the compressive and the tensile strengths is $\sigma_{ci}/\sigma_{ti} \cong 5$, which is low for granitic rocks. Common values for granites are σ_{ci}/σ_{ti} = 12-18 (Descoeudres, 1989). The rocks prevailing at Deriner site are therefore rather soft considering their lithologic origin, most probably due to weathering attributed to thermal water circulations.

2.2 *Comparison with granitic rocks from literature*

Based on the UCS and tangent moduli of the rock, Deere and Miller (1966) suggest a classification scheme for intact rocks that can be useful in determining whether or not the properties measured at the Deriner Dam site are commonly encountered in practice. According to Deere and Miller, the rock is divided into one of the five categories of UCS (σ_{ci}), and into one of the three categories of Modulus Ratio ($MR = E_{Si}/\sigma_{ci}$).

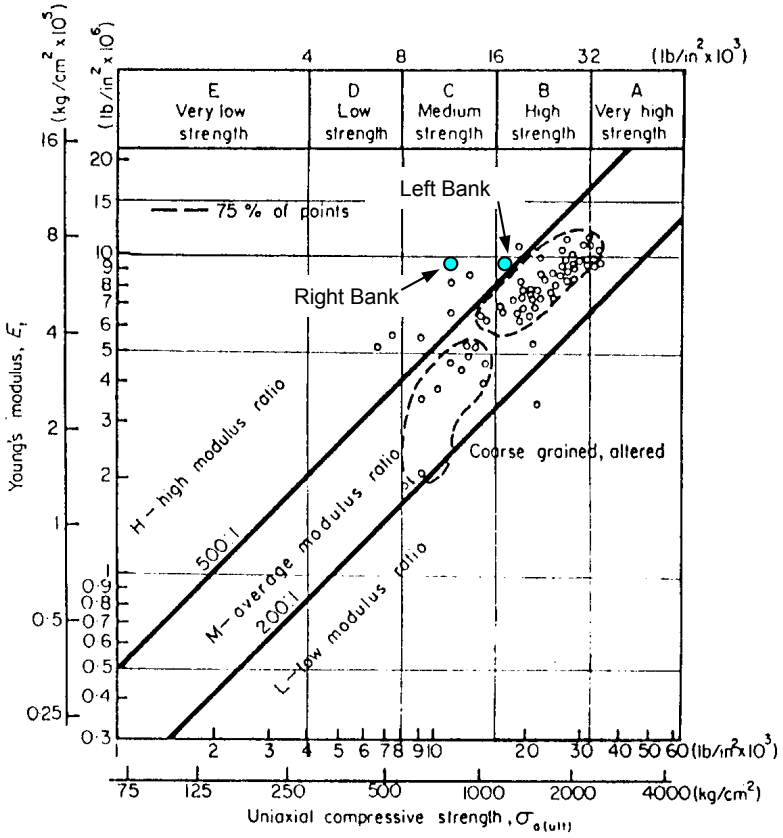

Figure 3: Engineering classification for intact granitic rock (Deere and Miller, 1966). (Note: 1 MPa = 10 kg/cm^2).

Figure 3 represents this classification scheme for granitic rocks. Most of the data, gathered from granite samples extracted from 80 different sites, fall into the "*medium modulus category*". In contrast, the rocks encountered at the Deriner Dam site exhibit quite a high stiffness and fall into the categories CH and BH for the right and left banks, respectively, thus in the "*high modulus*" range. The plot of Figure 3 shows therefore that these rocks are rather soft and stiff, which can indicate micro-cracking.

2.3 *Joint sets*

A complete description of a joint set is usually given by its geometrical characteristics and its mechanical properties. The geometrical characteristics comprise orientation, spacing, size and aperture, and the most useful mechanical property is the shear strength.

Joint orientation

Ideally, a thorough joint survey should provide enough data to enable one to define, for each set, a reliable value for the mean orientation and the spherical probability density function best describing the variability of the orientation of each joint around the mean orientation of the set. A large variability of the orientation of the joints has been encountered at the Deriner Dam site and one has to be aware that the values listed in Table 3 represent average values exhibiting large scattering. Although this seems disturbing when one wants to perform accurate and sound engineering analyses, it also leads to the conclusion that the rock blocks that are formed by these joints are generally interlocked so that no large unstable rock volumes are to be expected.

Table 3: Summary of mean orientation of joint sets in right and left banks.

Set	**Left bank**	**Right bank**
A	051 / 85	032 / 89
B	154 / 87	296 / 87
C	276 / 29	245 / 38
D	117 / 35	093 / 47
E	337 / 49	331 / 37

Joint shear strength

A series of 24 direct shear tests was performed on core samples with joints, following the ISRM recommendations, 23 of which were performed on granodiorite cores and only one on diabase. Three properties have been measured: the peak shear strength, the residual shear strength and the reverse residual shear strength (Table 4). This latter, which consists in the measurement of the residual shear strength after reversing the direction of shearing, so that the values of friction angles obtained are not affected by misalignment of the joint plane with the shearing plane. Four different normal stresses were applied, namely 0.5, 1.0, 2.0 and 4.0 MPa. The tests were evaluated with and without area correction, meaning that the stresses were computed once with the initial sample area, and once with the effective area taking into account the shear displacement.
It was attempted to group the results according either to the location of the cores or to the appearance of the joint surface. Unfortunately such an attempt to classify the measurements is limited by the small number of tests per group. A possibly awkward result of one of the tests can therefore have a very strong influence, leading to biased estimates of the shear parameters.

Table 4: Joints failure envelopes parameters as derived with the shear tests results.

	Without area correction				With area correction		
	Peak		Residual	Reverse Residual	Peak		Residual
	c_d [MPa]	ϕ_{pd} [°]	ϕ_{rd} [°]	ϕ_{rrd} [°]	c_d [MPa]	ϕ_{pd} [°]	ϕ_{rd} [°]
Left bank	0.59	48.5	39.5	30.5	0.60	48.5	39.5
Right bank	0.38	47.0	35.0	28.5	0.65	43.5	36.5
Average	0.43	47.5	36.0	29.0	0.67	44.5	37.0

The peak and residual failure parameters are slightly higher in the left than in the right bank, which is probably not meaningful considering the small number of tests run. The evaluation of the results with area correction tends to slightly increase the cohesion and slightly decrease the peak friction angle; but it has no effect on the residual friction angle. It is interesting to note that the reverse residual friction angles are almost constantly lower than the residual angles, which means that further shearing from the so-called residual state lowers the friction even more. In addition to that, a cautious interpretation of the residual values shall be made as they might be affected by the test procedure.
At Deriner site, the residual joint strength parameters were taken as follows:

- cohesion c_r=0 MPa,
- friction angle ϕ_r=40°.

3 OVERFLOW SPILLWAYS

3.1 *Introduction*

In order to evacuate the floodwater safely, two gated spillway tunnels have been designed with maximal capacity of 2250 m^3/s. The overflow spillway tunnels start with a transition zone (Figure 4) over which the tunnel shape (horseshoe) and size (12 m width and 18 m height) is decreasing to a circular section 10 m of diameter. The first part of the tunnel is in curvature with a radius of 180 m and a central angle of 62° (Figure 1).

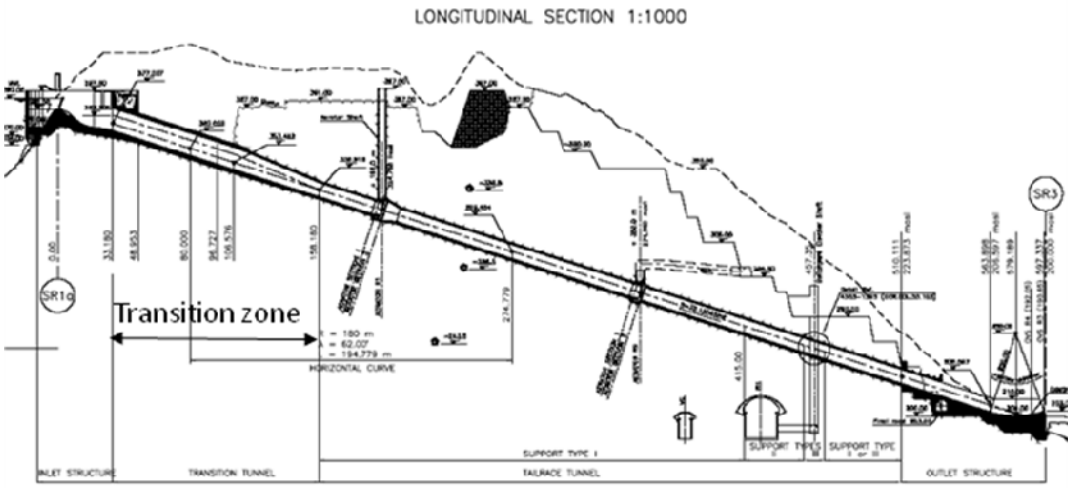

Figure 4: Longitudinal section of the overflow spillway on the right bank.

The overflow spillway transition tunnel on the right bank is shallow over a distance of about 50m. At the beginning, overburden is about 20 m and the pillar roughly 15 m wide with a huge excavation section (12 m wide and 18 m height). Thus, a special attention has been given to the excavation of this shallow tunnel area.

In addition to that, on the right bank, a persistent low strength C joint set (dip direction/dip angle 250/45) has been encountered (which is actually rather a fault having almost the same dip and dip direction as joint set C) that dips into the excavation at a highly unfavourable angle. The fault was responsible for the failure of the slope below the overflow spillway platform and above the power intake area where an anchored wall was constructed. In order to achieve a minimum short term factor of safety of 1.2, 200 pre-stressed anchors have been installed in the slope above the overflow spillway and the power intake.

3.2 *Geological in-situ conditions*

The generalised Hoek-Brown failure criterion (2002) has been evaluated with the following material parameters:

- Geological Strength Index (GSI) = 45,
- Unconfined Compressive Strength = 80 MPa (Right Bank),
- m_i = 29±3 (recommended by Hoek-Brown for granodiorite rock type), a mean value of 29 has been assumed,
- Disturbance factor = 1.0 (industrial blasting, after Hook et al. (2000), corresponding to very poor quality blasting results in a hard rock tunnel, resulting in severe local damage, extending 2 or 3 m in the surrounding rock mass),
- General normal stress range applicable for tunnel excavation σ_3 from 0 to 1.5 MPa. For this specific case, σ_3 = 0-0.5 MPa above the overflow spillway tunnel, close to the portal.

The Mohr-Coulomb strength parameters have been adjusted to fit the normal stress range prevailing in the dam abutment area (RockLab, 2002). Therefore, the parameters used to describe the rock mass in the analysis are:

- cohesion c_m = 0.35 MPa
- friction angle $\phi_m = 40°$

The assumed parameters tend to decrease the difference between Mohr-Coulomb and Hoek-Brown criteria at low stress states, which is prevailing in the close vicinity of the tunnel.

Deformability of the rock mass

An accurate and reliable estimation of the deformability of the rock mass is of utmost importance since it is used for the design of the overflow spillway structure. At Deriner site, the deformability of the rock mass has been assessed by static (plate-load and dilatometer tests) and dynamic in-situ tests and from empirical correlations (Bienawski, 1989; Serafim & Pereira, 1983; Barton, 2000).

The measured values of the modulus suggest that the vertical direction is stiffer than the horizontal ones. The overall moduli of deformation, recommended at the time of the Final Design (last step before Construction design) for the rock mass are summarized in Table 5.

Table 5: Design values for the modulus of deformation of the rock mass

E_m [GPa]	Horizontal direction	Vertical direction
Left bank	7	10
Right bank	11	8

Based on Table 5, an average value of the modulus of deformation E = 9 GPa has been used for the analysis of the dam and the powerhouse. In the course of the excavation works, a back-analysis has been carried out for the open-air excavations (cable crane and dam) and underground excavations. The back-calculated values range between 3.5 GPa and 7 GPa .

Referring to Hoek et al. (2002) one can estimate the modulus of deformation for the rock mass based on the GSI-approach:

$$Em(GPa) = \left(1 - \frac{D}{2}\right)\sqrt{\frac{\sigma_{ci}}{100}}\,10^{(GSI-10)/40} \quad \text{for } \sigma_{ci} \le 100MPa \tag{1}$$

$$Em(GPa) = \left(1 - \frac{D}{2}\right)10^{(GSI-10)/40} \quad \text{for } \sigma_{ci} > 100MPa\,. \tag{2}$$

In Deriner case, with D=0.5 ÷ 1.0 and the corresponding values of GSI for the areas under consideration in the left and right banks, it is obtained:

E_m = 5 ÷ 8 GPa for the left bank, and

E_m = 3 ÷ 5 GPa for the right bank.

Thus, based on the above, it has been decided to carry out a first calculation with E = 7 GPa and then to study the effect of a decrease of the E_m-modulus on the tunnel and slope behaviour.
Furthermore, Poisson's ratio is fixed, based on the literature, equal to $\nu = 0.25$. This value is theoretical as it applies to the rock mass and since, of course, no test exists to demonstrate the validity of such a value.

3.3 *Finite element modelling*

The analysis was carried out using the Finite Element (FE) program Z-SOIL.PC, which is a continuously upgraded geotechnical, foundation and underground flow engineering software. The elasto-plastic constitutive models introduced in Z-SOIL correspond to the most commonly used in practice: the Tresca, Mohr-Coulomb, Rankine, Drucker-Prager-Cap, and Cam-clay models for soil, multi-laminate for layered media and schist, Hoek-Brown models for rock, Menétrey-Willam (with softening) for concrete (http://www.zace.com).

A plane strain analysis that requires 2D modelling, has been carried out, considering a vast region in the horizontal direction extending from –800 m to +500 m from the tunnel axis. It must be noted that the temporary support is introduced in calculations after 30% of stress relaxation. Thus, the remaining 70% of deformation of a certain sub-step plus of course each following sub-steps introduce forces into the temporary support.
A general view of the finite element mesh and a zoom of the tunnel area are represented in Figure 5. The FE analysis was carried out introducing beam elements in the numerical analysis after the corresponding tunnel sequence excavation.

The C-fault mentioned earlier has been included in the analysis using contact elements. Shear strength parameters for the C-fault have been derived from a back-analysis. The deformation modulus of this weak zone is adopted to be the same as the surrounding rock. Moreover, the existing pre-stressed anchors have been included in the analysis with corresponding force of 1'860kN/anchor. The results of the numerical analysis are given in terms of deformations (see example in Figure 6), stresses in the surrounding rock, a plastic zones developed in the rock and internal forces in the temporary support.

The surrounding dam excavation has been simulated in one time step starting from the initial in-situ stress state. The K_0-value has been investigated in a separate study and is kept constant for all calculations (K_0=1.5).

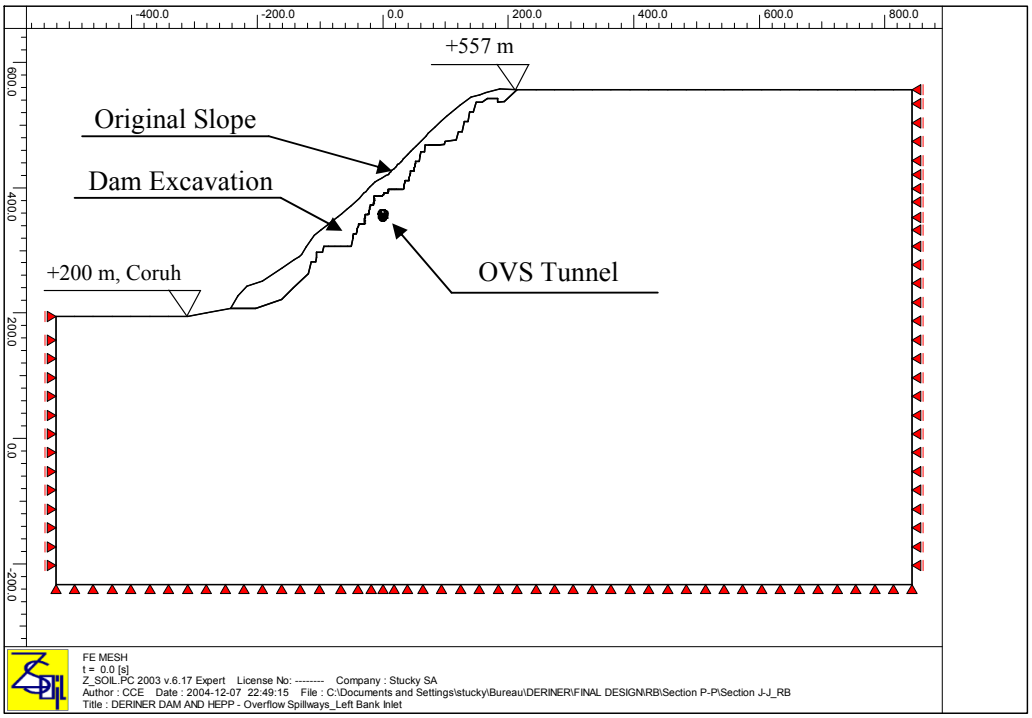

Figure 5: Extension of the area considered in the analysis.

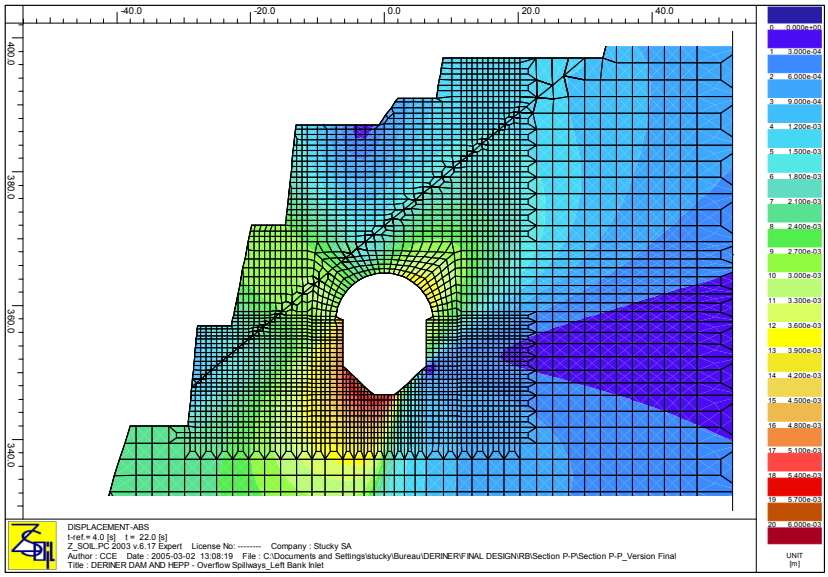

Figure 6: Maximal displacement due to tunnel excavation.

Based on a preliminary analysis of the rock support, carried out using standard rock mass classifications (RMR, GSI, and Q methods), a tunnel support is pre-designed as:

- INP 220 steel ribs, spacing 1.0 m,
- shotcrete 12 cm thick, which is then increased to get a temporary vault 35 cm thick,
- in the walls, the shotcrete is 12 cm thick, and reinforced with wire mesh.
- systematic bolting spaced 1.5 x 1.5 m (2.25 m^2/pce), L=5 m. Due to presence of the C-fault (Figure 6) on the valley side of the tunnel length of the rockbolts has been increased to 9 m and spacing 1 x 1 m (Figure 8).

Based on the above, it was confirmed that the overflow spillway can be excavated with a necessary structural safety of the tunnel temporary support.

3.4 *Rock wedge stability analysis*

In addition to the above presented analysis, a rock wedge stability analysis has been carried out. The rock wedge stability analysis is based on the block theory developed by Goodman & Shi (1985). The method consists in a geometrical analysis allowing to define systematically the most critical combination of joint sets leading to falling or sliding of the removable wedges with respect to the excavation surfaces, such as the roof, walls, edges or corners of the tunnel. This analysis is performed using the program UNWEDGE (Rocscience Inc., 2004), which is specifically adapted for this type of analysis. A similar study has been carried out exhaustively for the powerhouse with satisfactory results.

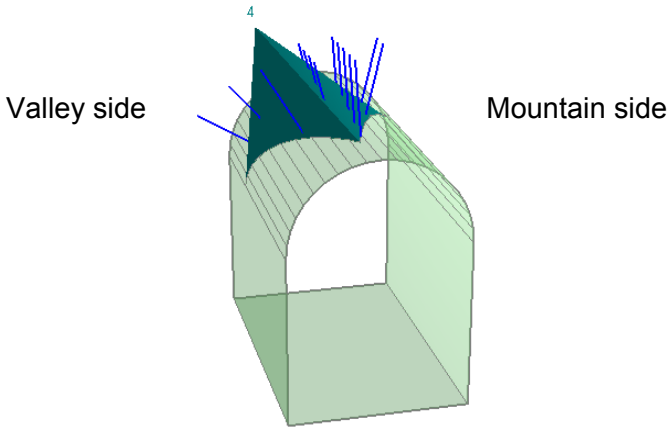

Figure 7: Right bank, overflow spillway tunnel: potentially unstable rock wedge formed by joints A – B – D (3D view).

The rock wedge stability analysis for the right bank is carried out for all possible combinations of joint sets listed in Table 3 and the C-fault. In the analysis, the foreseen systematic rockbolts, 1.5 m spacing in the tunnel roof and in the tunnel pillar has also been introduced. The overflow spillway tunnel on the right bank is defined by the following orientation: dip/dip direction=18/352 ÷ 360. The smallest safety factor of 1.4 is calculated for a wedge formed by the joint sets A – B – D with volume of 78.1 m^3 (Figure 7). Since the analysis is carried out taking into account only rockbolts as support, the obtained safety factor is considered as enough for temporal safety. The introduction of shotcrete would increase considerably the safety factor.

3.5 *Rock support and construction*

Based on the above presented analysis, the rock support has been assumed as illustrated in Figure 8. For successful overflow excavation works, it was of fundamental importance that blasting and excavation are very carefully executed in order to prevent from damage of the surrounding rock mass. To minimize over-break, the direction of the blast-holes was carefully selected and the borehole deviation and the charging operation were controlled. Since the tunnel is highly inclined, the excavation started with benches of 1 m high and then heading with a round of 3 m.

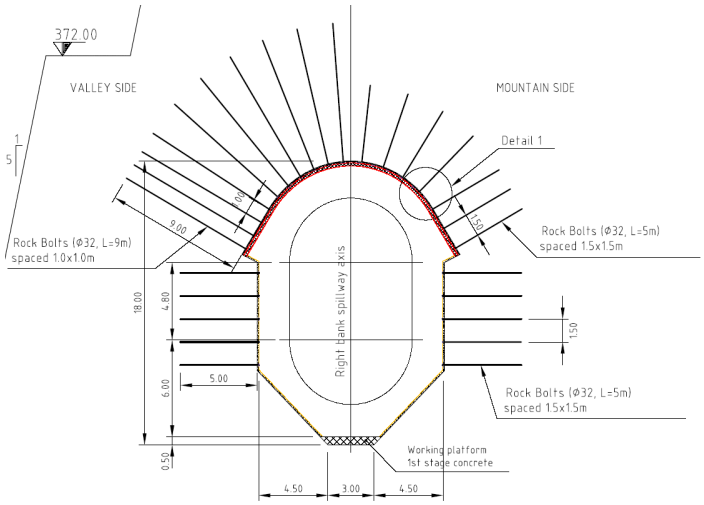

Figure 8. Rock support of the overflow spillway on the right bank.

Figure 9. Overflow spillway on the right bank: photos made during construction.

For the purpose of the tunnel excavation, a special winch on rails has been developed, allowing transport of the excavated material. It should be noted that the excavation of the overflow spillway has been successfully carried out (Figure 9) without any stability problem in spite of a quite complex geometry of the tunnel and quite difficult geological conditions.

4 CONCLUSION

The rock mass at the Deriner site is mainly composed of weathered granodiorite intruded by diabase dykes, which are generally suitable for the foundation of an arch dam. Furthermore, the upper layer of the rock is decompressed and heavily jointed, which means that it has to be excavated so as to ensure sound rock for the dam foundations.
The paper presents geotechnical consideration and design of the overflow spillway tunnels excavation and rock support. The overflow spillway tunnels start with a horseshoe shape transition zone over a length of about 50 m with a very shallow coverage (about 20 m and 15 m in pillar). In addition, the tunnel is parallel to the slope, which is highly unfavourable. The design of the tunnel excavation and the rock support is based on the classical rock classifications (GSI, RMR and Q) followed by sophisticated Finite Element analyses and a structural discontinuity analysis.
The design of the rock support and the excavation methodology has been confirmed by successful overflow spillway excavation on the site.

ACKNOWLEDGEMENT

The authors are grateful to the General Directorate of State Hydraulic Works (DSI), Ministry of Environment and Forestry of Turkey for allowing publication of this paper.

5 REFERENCES

Bieniawski, Z. T. 1989. *Engineering rock mass classifications*. John Wiley &Sons, New York.
Barton, N., 2000. *TBM Tunnelling in jointed and faulted rock.* Balkema, Rotterdam.
Descoeudres, F. 1989. *Mécanique des roches*, Lausanne: Ecole Polytechnique Fédérale de Lausanne.
Deere, D. U. & Miller R. P. 1966. *Engineering Classification and Index Properties for Intact Rock* ;Tech. Rept. No. AFWL-TR-65-116, Air Force Weapons Lab., New Mexico, 1966.
Goodman, R. E., & Shi, G. 1985. *Block theory and its Application to Rock Engineering*, Prentice-Hall.
Hoek, E., Kaiser, PO. K., & Bawden, W. F. 2000. *Support of Underground Excavations in Hard Rock*, Balkema, Roterdam.
Hoek, E., Carranza-Torres, C., & Corkum, B. 2002. *Hoek-Brown failure criterion – 2002 edition*. Proceedings of 5th North American Rock Mechanics Symposium, Toronto, 1:267-273.
RocLab – *Rock mass strength analysis using the Hoek-Brown failure criterion*, User's guide, Rocscience Inc. 2002.
Serafim, J. L., & Pereira, J. P. 1983. *Consideration of the Geomechanical Classification of Bieniawski*, International Symposium of Engineering Geology and Underground Classifications, Lisbon, Portugal, 1133-1144.
Unwedge Theory Manual, *Factor of Safety Calculations*, Rocscience Inc., 2004.